

pH gradients are not associated with tip growth in pollen tubes of *Lilium longiflorum*

M. D. Fricker¹, N. S. White¹ and G. Obermeyer^{2,*}

¹Department of Plant Sciences, University of Oxford, South Parks Road, Oxford, OX1 3RB, UK

²Institut für Pflanzenphysiologie, Universität Salzburg, Hellbrunnerstrasse 34, 5020 Salzburg, Austria

*Author for correspondence (e-mail: gerhard.obermeyer@sbg.ac.at)

SUMMARY

The cytoplasmic pH of growing pollen tubes of *Lilium longiflorum* Thunb. was measured using the pH-sensitive fluorescent dye 2',7'-bis-(carboxyethyl)-5(6')-carboxyfluorescein and confocal fluorescence ratio imaging. The average cytoplasmic pH in the clear zone of the pollen tube tip was pH 7.11, and no consistent pH gradients were detected in the clear zone, averaging around -1.00 milli pH unit μm^{-1} , or along the first 50 μm of the tube (3.62 milli pH units μm^{-1}). In addition, no correlation was observed between the absolute tip cytoplasmic pH or the pH gradient and the pollen tube growth rates. Shifts of external pH to more acidic pH values (pH 4.5) caused a relatively small acidification by 0.18 pH units, whereas a more alkaline external pH >7.0 caused a dramatic increase in cytoplasmic pH and growth stopped immediately. Stimulation of the plasma membrane H^+ -ATPase by fusicoccin, resulted in an increase of tube growth but no change in cytoplasmic

pH. On the other hand, vanadate (250-500 μM), a putative inhibitor of the pump, stopped tube growth and a slight cytoplasmic alkalinisation of 0.1 pH units was observed. Vanadate also arrested fusicoccin-stimulated growth and stimulated an increased alkalinisation of around 0.2 pH units. External application of CaCl_2 (10 mM) caused a small acidification of less than 0.1 pH units in the clear zone, whilst LaCl_3 (250 μM) caused slight and rather variable perturbations in cytoplasmic pH of no more than 0.1 pH units. Both treatments stopped growth. It was inferred from these data that tip-acid cytoplasmic pH gradients do not play a central role in the organisation or maintenance of pollen tube tip growth.

Key words: BCECF, Confocal microscopy, Cytoplasmic pH gradient, *Lilium longiflorum*, pH regulation, Pollen tube tip growth, Ratio imaging

INTRODUCTION

Developing pollen grains are one of a number of ideal model systems to study tip growth and polarised secretion, as the secretion process is spatially organised in the clear zone (CZ) at the tip of the tube. Moving back from the tip, there are overlapping domains enriched progressively in secretory vesicles, dictyosomes, endoplasmic reticulum, mitochondria, and subsequently larger organelles carried on actin bundles in the rapidly streaming cytoplasm 10-30 μm behind the tip (Reiss and Herth, 1979; Lancelle and Hepler, 1992). Large numbers of secretory vesicles, in the range of 1,000-3,000 minute^{-1} per tube, are transported into the tip region of the tube where they fuse with the plasma membrane and deposit pectin to form the extending cell wall (Picton and Steer, 1983; Van der Woude et al., 1974). Whilst the cytoskeleton is central to the organisation and maintenance of localised secretion (Pierson and Cresti, 1992), a number of ion transport processes are also closely associated with control of polarised tip growth (Feijó et al., 1995; Derksen et al., 1995). Electrical currents circulate between the tube and the pollen grain. The majority of the current is initiated by proton extrusion from the pollen grain, where there is a high density of plasma membrane (PM) H^+ -ATPase (Obermeyer et al., 1992), and re-enters mainly as K^+ along the length of the

tube (Weisenseel and Jaffe, 1976). A smaller component of the current is carried by Ca^{2+} entering the very tip of the tube (Kühtreiber and Jaffe, 1990; Pierson et al., 1995). This localised Ca^{2+} influx is associated with a tip-focussed gradient in cytosolic free Ca^{2+} concentration ($[\text{Ca}^{2+}]_{\text{cyt}}$) of varying magnitude (0.7 to 5 μM at the tip) and extent, reaching resting levels 10 to 70 μm behind the tip (Nobiling and Reiss, 1987; Obermeyer and Weisenseel, 1991; Rathore et al., 1991; Pierson et al., 1995). The $[\text{Ca}^{2+}]_{\text{cyt}}$ gradient appears to be critical for polarised growth as high Ca^{2+} zones are absent in non-growing tubes (Rathore et al., 1991; Miller et al., 1992), and calcium channel blockers dissipate the Ca^{2+} gradient and inhibit growth (Obermeyer and Weisenseel, 1991; Malhó et al., 1995). High $[\text{Ca}^{2+}]_{\text{cyt}}$ may influence a number of key components in the secretory system directly, or indirectly via a parallel gradient in the distribution of the high-affinity Ca^{2+} -binding protein calmodulin (Haußer et al., 1984; Tirilapur et al., 1994). For example, elevated Ca^{2+} causes fragmentation of actin (Kohno and Shimmen, 1987), kinetic regulation of transport motors (Heslop-Harrison and Heslop-Harrison, 1989; Putnam-Evans et al., 1989; Cai et al., 1996), and vesicle fusion promoted by the members of the annexin family of Ca^{2+} -dependent phospholipid binding proteins (Blackbourn et al., 1991) that are localised to the tube tip (Blackbourn et al., 1992).

Recently, a gradient in cytosolic pH (pH_{cyt}) was reported during tip growth of rhizoids from *Pelvetia fastigiata* which increased by 0.3–0.5 pH units from pH 7.15 at the tip over about 50 μm (Gibbon and Kropf, 1994). As treatment with permeant weak acids both abolished the pH-gradient and halted growth, it was suggested that pH-gradients may act in concert with Ca^{2+} -gradients to control polarised secretion in this system (Gibbon and Kropf, 1994). Given the importance of pH in modulating several elements involved in pollen tube tip growth, such as cytoskeletal structures (e.g. Tiwari and Suprenant, 1994) and the Ca^{2+} -binding affinity of annexins (Blackbourn et al., 1991), it is important to test whether pH-gradients are a universal feature of tip growing systems. The evidence to date is equivocal; cytoplasmic pH-gradients were not associated with tip growth in root hairs (Herrmann and Felle, 1995), but have been reported for fungal hyphae showing an acidified tip (McGillviray and Gow, 1987; Turian et al., 1985). Published information of cytosolic pH in pollen tubes is scarce. Measurements using absorbance dyes indicate highly acidic regions in the apical zone of pollen tubes (Turian, 1981), although this signal may well be derived from dye in the organelles. A similar low pH at the tip is cited from unpublished measurements using fluorescence imaging of the pH indicator BCECF (U. K. Tirlapur, cited by Pierson and Cresti, 1992). Recently, preliminary results were reported showing the tip pH was slightly below pH 7.0 and pH gradients were present in a number of growing tubes (Feijó et al., 1995).

In this study we have used dual-excitation confocal ratio imaging of the pH-sensitive dye BCECF to quantify pH_{cyt} in pollen tubes of *Lilium longiflorum* and assess whether cytoplasmic pH gradients exist that can be correlated with tip growth.

MATERIALS AND METHODS

Plant material and microscopy

Flowers of *Lilium longiflorum* were purchased locally. Pollen grains were collected 2 days after dehiscence, and washed briefly in 5% ethanol to remove most of the pollenkitt. Pollen were concentrated by centrifugation (1,000 g, 1 minute) and resuspended in culture medium (10% (w/v) sucrose, 1.6 mM H_3BO_3 , 1 mM KCl, 0.1 mM CaCl_2 , pH 5.6) to a final density of approximately 3,000 grains ml^{-1} . Germinating grains were incubated in 1–5 μM 2',7'-bis-(carboxyethyl)-5(6')-carboxyfluorescein (BCECF-AM) from a 2 mM stock solution in ethanol, for 2–3½ hours. Pollen tubes only took up dye after emergence from the grain and were allowed to grow to 200–400 μm in length (~30–60 minutes post-emergence). Ethanol concentrations up to 0.5% had no detectable effect on pollen germination and tube growth. Samples of 100–300 μl germinated pollen were washed gently by centrifugation to remove extracellular indicator and transferred to coverslips (no. 1½, Chance-Popper, Warwick, UK) previously coated with 0.01% (w/v) poly-L-lysine for 5 minutes. Coverslips were mounted in open perspex chambers using silicone grease and viewed using a Nikon Diaphot inverted microscope with either a Zeiss $\times 25$, 0.8 NA multi-immersion lens or a Nikon $\times 60$, 1.4 NA oil immersion lens. Chemicals were carefully added to the perspex chamber from stock solutions to give final concentrations of 250–500 μM vanadate, 10 μM fusicoccin, 10 mM CaCl_2 , 250 μM LaCl_3 , 20–40 μM FCCP, and 10 μg ml^{-1} nigericin, respectively. Room temperature was maintained at 18–20°C giving typical growth rates of around 4–6 μm minute^{-1} .

Confocal fluorescence ratio imaging

Dual-excitation confocal ratio measurements used a confocal laser scanning microscope (CLSM) based around a Bio-Rad MRC600 attached to a Nikon Diaphot inverted microscope with modification of the excitation path to receive co-aligned beams at 488 nm (25 mW argon ion, ILT Ltd), 442 nm (11 mW HeCd, Omnichrome) and 633 nm (3.5 mW HeNe, Spekra Physics) (Fricker and White, 1992; Fricker et al., 1994).

Confocal fluorescence optical sections were collected in the mid focal plane of the pollen tube tip using sequential excitation at 442 nm and 488 nm, and emission at 540 ± 15 nm. Computer controlled electronic shutters ('Uniblitz', Vincent Associates, New York) were used to switch between excitation wavelengths. Neutral density filters were used to balance roughly the intensity of the two beams. Bright field transmission images were collected with illumination from the 663 nm laser using a non-confocal transmission detector and fibre-optic coupling to the second MRC 600 channel immediately after each ratio pair.

Each wavelength image was typically collected over 768×96 pixels, with a pixel spacing of 0.183–0.25 μm . The sampling rates depended on the number of image lines collected and the number of frames integrated (typically 2–4 per wavelength). Acquisition of each wavelength pair took about 1–2 seconds and sampling was repeated at 5 to 20 second intervals.

Image processing and data analysis

To visualise changes in pH_{cyt} , log ratio images were calculated pixel by pixel for the 488 nm image divided by the 442 nm image, after subtraction of average background value, and median filtered using a 3×3 box. The tube was segmented using a threshold set at 50% of the average tip intensity in the 442 nm image. Additional masking was used to exclude regions where the signal was approaching saturation, defined where the mean was approximately 2 s.d. units below 255 (typically a grey level value of 200) in either wavelength image. Final ratio images were pseudocolour coded using look-up tables where the ratio was represented by 255 levels of fully saturated colour ranging from blue (typically pH 6.0) through green to red (typically pH 8.0).

To extract quantitative data, pixel values were averaged over circular regions (20–40 μm^2) manually located on each wavelength image. A single ratio value was calculated from the average 488 intensity divided by the average 442 intensity for this region, after subtraction of the corresponding image backgrounds. Alternatively, a semi-automated protocol was developed to extract data from a number of regions along the pollen tube. A cursor was used to draw a transect along the tube and the intensities were averaged over 8–24 pixels normal to the track for both wavelengths. Sampling was repeated for each (x,y)-image in the time course and data from each transect written into successive lines of a (l,t)-(length,time)-image, where l is the length from the tip of the tube, using a small 'C' program run from within MPL. (l,t)-ratio images and threshold masking were calculated as described for (x,y)-images. The position of the leading edge in each transect moved across the image with increasing time. The slope of this moving boundary (dl/dt) gave the growth rate. The position of the boundary was used as a reference to align each transect with respect to the growing tip. Vertical transects across the aligned (l,t)-image provided direct access to the change in ratio for a specified longitudinal region of the pollen tube (Fricker et al., 1994, 1997).

Calibration of ratio values

In vitro calibration was performed using 40 μM BCECF in a pseudo-cytoplasm (100 mM KCl, 10 mM NaCl, 1 mM MgSO_4 , 10 mM MES, 10 mM Hepes, adjusted with Tris base to the desired pH) supplemented with 25% ethanol. In situ calibrations were made after permeabilisation of the plasma membrane with either nigericin (10 μg ml^{-1} final concentration from a 10 mg ml^{-1} stock solution in ethanol) in the presence of KCl (40–120 mM) or FCCP (10–30 μM final concentration from a 1 mM stock solution in ethanol). Then 25 mM

Mes/BTP, pH 6.0, in culture medium was added to a final concentration of 2 mM to set the external pH (pH_o) to around pH 5.5-6.0. This was followed by addition of 25 mM BTP-Cl, pH 8.0, in culture medium which raised pH_o to around 7.5. The actual pH_o values obtained by these treatments depended on the previous additions in each experiment and were determined in parallel experiments using a pH electrode. Using nigericin, pH_{cyt} was estimated from pH_o assuming an average internal K^+ concentration of 117 mM (Obermeyer and Blatt, 1995) and that nigericin equilibrates pH according to the following equation (Chaillet and Boron, 1985):

$$[H]_i/[H]_o = [K]_i/[K]_o. \quad [1]$$

Calibration curves were generated for each block of experiments (when the instrument settings were kept constant) according to the following equation:

$$[H]_i = K_{app} \cdot (R_{max} - R) / (R - R_{min}), \quad [2]$$

where R_{min} and R_{max} are the minimum and the maximum ratio value measured after the addition of ionophores plus low and high pH, respectively, and K_{app} depended on the K_d and the fluorescent properties of the bound and free form of the dye at 442 nm. With 442 nm being the isosbestic point $K_{app} = K_d$. Where possible, individual calibrations were used for each experiment following the recommendation of Chaillet and Boron (1985). If it was not possible to measure R_{max} directly, the value was extrapolated as $4.86 \times R_{min}$ from a single point calibration and reference to the range of the ratio measured in situ and in vitro. If neither calibration worked, then values were extrapolated from the calibration curve derived for each block of experiments.

Levels of dye compartmentalisation were estimated after permeabilisation of the plasma membrane with 100 μ M digitonin to release cytosolic dye. Release of dye from within the compartments was achieved with addition of 0.1% Triton X-100.

Post-processing and analysis was performed using MPLTM software (Bio-Rad Microsciences Ltd Hemel Hempsted) and some additional 'C' programs. Graphical and statistical analysis were performed using ExcelTM (Microsoft Corp.). Image montages were assembled using PhotoshopTM 3.0 (Adobe Systems Inc.) and printed on a dye sublimation printer (Kodak XLS 8600 PS).

Chemicals

BCECF-AM was obtained from Molecular Probes (Eugene, Oregon, USA). Fusicocin, FCCP, and nigericin were from Sigma. All other chemicals were from BDH Ltd (Poole, UK).

RESULTS

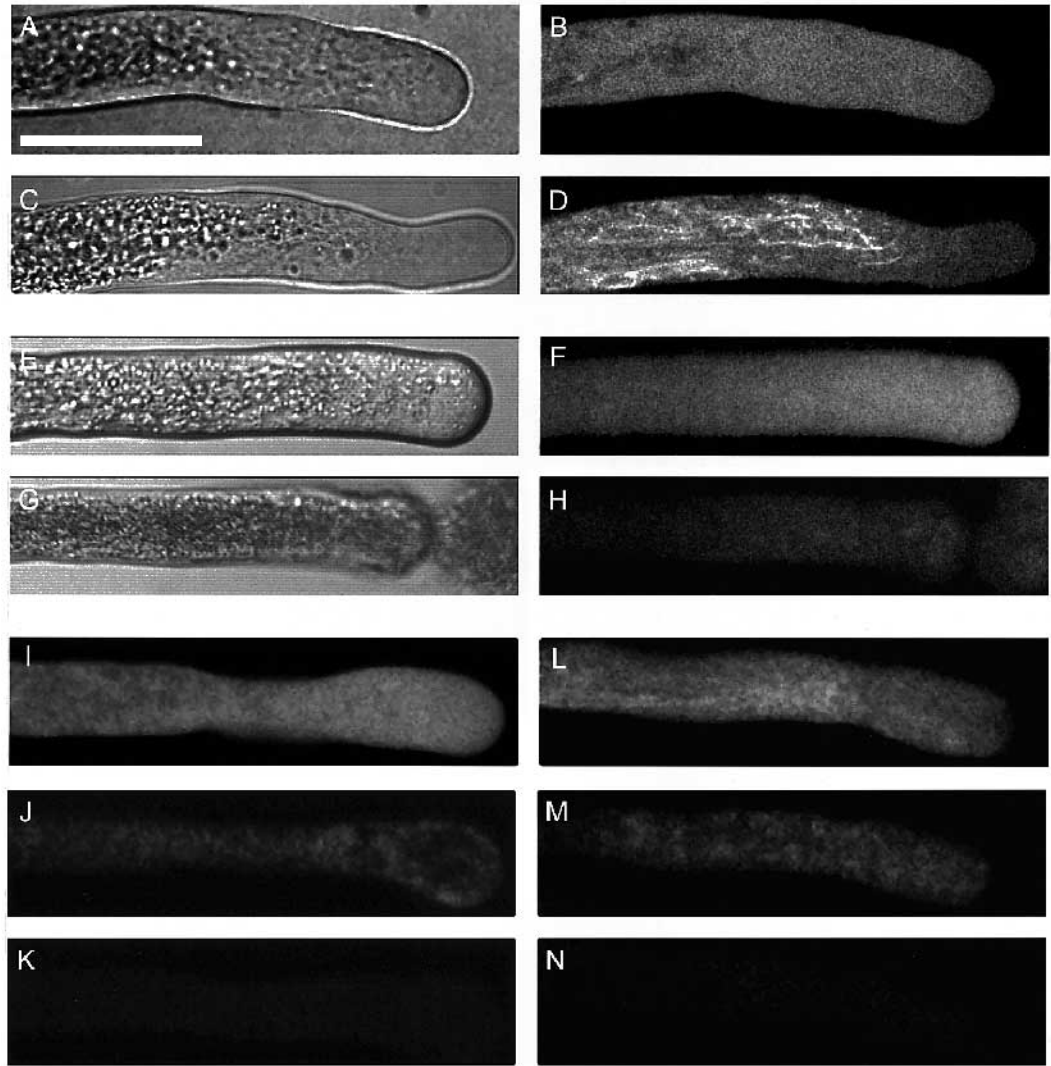
Pollen tubes of *Lilium longiflorum* were loaded with the pH indicator dye BCECF as the AM-ester. The overall tube morphology was visible in transmission images collected with illumination at 633 nm to avoid photobleaching (Fig. 1A), and fluorescence from dye hydrolysed internally was visualised in single optical sections with sequential excitation at 442 nm and 488 nm in the mid-plane at the tip of the growing tube. Excitation at 442 nm was near the isosbestic wavelength of BCECF so the emission signal depended only on the dye concentration and provided a map of the localisation of BCECF in the pollen tube (Fig. 1B). In most tubes, the fluorescence intensity in single optical sections with excitation at 442 nm was relatively homogeneous in the extensive clear zone (CZ) at the tip, with no obvious punctuate staining. The extent of the CZ was estimated from the transmission images and ranged from 10-30 μ m in length between different tubes. There was a slight decrease in signal in a zone near the extreme tip where the

secretory vesicles are concentrated (see also Fig. 5A). In the streaming cytoplasm other regions of apparently reduced fluorescence corresponded to dye exclusion from larger organelles that were clearly negatively stained (Fig. 1B). Occasional small bright fluorescent vesicles were visible even under these optimal loading conditions (Fig. 1B). In some tubes, and particularly with long loading periods, compartmentalisation was observed in a very dynamic tubular network extending throughout the streaming cytoplasm. The amount of dye compartmentalised in this tubular network increased with loading time; an extreme example is shown in Fig. 1D after 3 hours loading post-germination. Compartmentalised fluorescence was barely discernible after the normal 30-60 minute loading period (Fig. 1B). Furthermore, in tubes that burst during the experiment (e.g. Fig. 1E-H) the fluorescence spread rapidly from the tube as the vesicles surged forward. Fluorescence levels declined immediately within the tube (compare Fig. 1H taken 20 seconds after Fig. 1F) even though the tube was still clearly packed with vesicles in the transmission image (Fig. 1G). Given that dye compartmentalised in vesicles would interfere with quantitative analysis of cytosolic pH values, we measured the degree of compartmentalisation in evenly loaded pollen tubes (e.g. Fig. 1I) and tubes with readily discernible sequestration (Fig. 1L) after permeabilisation of the plasma membrane with digitonin. Cytoplasmic streaming ceased in the presence of digitonin over a 1-5 minute period and the vesicles invaded the CZ and tip region. Tubes lost turgor and shrank markedly concurrently with loss of the cytosolic signal. Compartmentalised dye was visible after this treatment as punctate vesicles or occasional strands within the tube (Fig. 1J and M). This remaining fluorescence disappeared almost completely with exposure to Triton X-100 to permeabilise all the intracellular membranes (Fig. 1K and N). Typically less than 12% of the fluorescence remained after digitonin treatment in evenly loaded tubes (11.6% for the tube shown in Fig. 1I and J), whereas levels reached up to 30-35% of the signal in tubes with strong compartmentalisation (31% for the tube shown in Fig. 1L and M). Only tubes with comparable loading to those shown in Fig. 1B,F or I were used in subsequent experiments.

Pollen tubes loaded with BCECF maintained vigorous cytoplasmic streaming and most tubes continued to grow under the illumination conditions used (e.g. Fig. 2) at a rate comparable to unloaded controls when measured in parallel at the same temperature (18-20°C) as the imaging experiments ($4.05 \pm 2.38 \mu$ m $minute^{-1}$ ($n=25$) for loaded compared to $5.22 \pm 2.6 \mu$ m $minute^{-1}$ for unloaded; $n = 157$). Typically tubes were imaged over a 10 minute period with sampling at 10-20 second intervals, although some experiments were continued for up to 1,000 seconds. Occasionally pollen tubes that showed rapid cytoplasmic streaming, but were not growing were also used to determine whether pH_{cyt} altered in non-growing tubes and, particularly, to see if changes in pH_{cyt} could be observed when such tubes were stimulated to grow using fusicocin (e.g. Fig. 8, see below).

To visualise changes in pH_{cyt} , the ratio image was calculated as I_{488}/I_{442} for each pixel after separate background subtraction at each wavelength and noise reduction using a median filter (e.g. Fig. 2B). The level of noise and/or compartmentalisation remaining was sufficient to give a speckled pattern to the ratio images (Fig. 2B), however, there was no obvious underlying trend in the CZ or further along the tube in the

Fig. 1. Intracellular distribution of BCECF in pollen tubes of *Lilium longiflorum*. The typical pollen tube morphology is shown in A from a non-confocal transmission image collected with illumination at 633 nm. The corresponding confocal optical section in the mid (x,y) focal plane after loading with BCECF as the AM-ester is shown with excitation at 442 nm. (B) Dye is evenly distributed in the cytoplasm in clear zone and excluded from organelles in the streaming cytoplasm. A single brightly stained vesicle is visible in the streaming cytoplasm. For comparison substantial compartmentalisation in a reticulate network was visible in the streaming cytoplasm and extending into the clear zone after prolonged loading (C and D). Occasionally during experiments, the pollen tube burst at the tip (E-H). In this case, the surge of vesicles towards the tip expelled most of the dye as a cloud that rapidly diffused away with little dye remaining in the tube (H) even though it remained packed with vesicles (G). Quantitation of the level of dye sequestration was possible after permeabilisation of the plasma membrane with digitonin. In an evenly loaded tube (I) 11.6% of the fluorescence remained after this treatment (J) and all this signal effectively dispersed after addition of Triton X-100 (K). In a tube showing extensive compartmentalisation (L), 31% of the dye remained after digitonin treatment (M). This dye was also released after Triton X-100 treatment (N). Bar, 25 μ m.



streaming cytoplasm. The pollen tube shown continued to grow at $4.7 \mu\text{m min}^{-1}$ during imaging and the cytoplasmic ratio values did not alter during the imaging period (3 time points are shown out of a total of 47 in Fig. 2B).

To calibrate the ratio values in terms of pH, in situ, the tube was exposed to the H^+/K^+ exchanger nigericin, and varying levels of external K^+ and pH_o to clamp pH_{cyt} to known values (Fig. 3). Rapid shifts in ratio were often achieved when clamping at low pH_{cyt} values (e.g. Fig. 3C and Fig. 2B'), especially if there was a slight delay before addition of the external K^+ to drive pH_i to R_{min} . Even after this treatment, the ratio was not completely uniform over the whole tube (see for example Fig. 2B' and B''). During calibrations, there were often dramatic structural changes at the tip (e.g. Fig. 2C) and small apparent shifts in either the amount of BCECF or its fluorescence properties, as judged by stepwise increases in fluorescence intensities with excitation at 442 nm particularly with addition of KCl (e.g. Fig. 3A). During calibration the rate of dye loss or photobleaching also increased (Fig. 3A). In a number of tubes it was possible to clamp pH_{cyt}

subsequently to higher values (e.g. Figs 2B'' 3, 8E), but many tubes burst when pH_o was alkalinised.

In situ calibration values from one block of 17 experiments are plotted in Fig. 3C. The solid line represents a fit to the data using equation 2 with a pK_a of 7.2. The open symbols are from in vitro calibration solutions in a simple ionic medium supplemented with 25% ethanol to increase the hydrophobicity (see Russ et al., 1991) and measured with the same instrument settings. A similar set of calibration data were obtained for each separate block of experiments. The dynamic range of the ratio was about 5-fold between R_{min} and R_{max} . In the calibration shown in Fig. 3A,B the 90% confidence limits on the ratio correspond to a minimum detectable pH change of less than 0.1 pH units for a circular area of $28 \mu\text{m}^2$ containing around 800 pixels. In the experiment shown in Fig. 2, the calculated value of pH_{cyt} during the low and high pH calibrations was pH 5.75 (Fig. 2B') and pH 7.45 (Fig. 2B''). The average tip pH_{cyt} was estimated as pH 7.2 based on the calibration values at the tip for a circular area of 8 μm diameter. The maximum

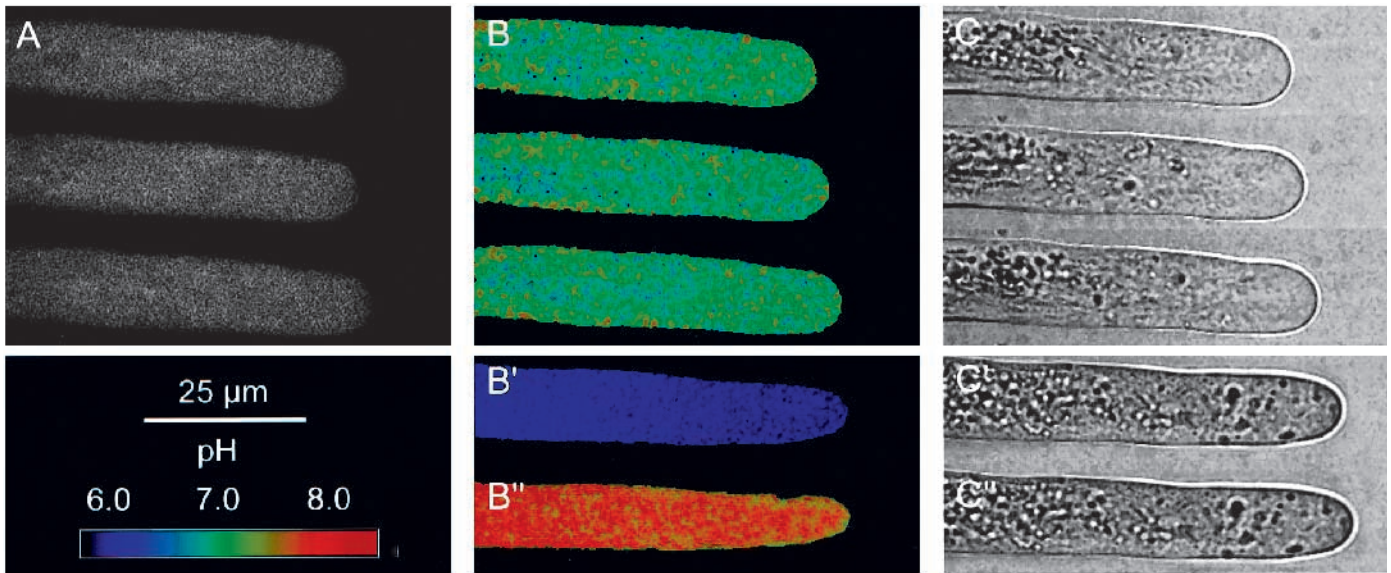


Fig. 2. Dual-excitation confocal ratio imaging of cytoplasmic pH in growing pollen tubes of *Lilium longiflorum*. Single optical sections in the mid (x,y) focal plane of a growing pollen tube were collected sequentially with excitation at 442 nm (A) and 488 nm (not shown) after loading of BCECF as the AM-ester. A non-confocal, bright field transmission image was collected after the ratio pair with illumination at 633 nm (C). The time-interval between image sets was 20 seconds. Ratio images were calculated pixel by pixel after subtraction of the image background at each wavelength and masking at a grey-level value of 36 in the 442 nm image. Values above 200 were also masked in both images to exclude pixels approaching saturation. Images in B have been median filtered with a 3×3 box. At the end of the experiment, the internal pH was calibrated in situ using nigericin, high K^+ (107 mM) and low pH (B') followed by high pH (B''). The conversion from ratio values to pH derived from the in situ calibration is indicated on the inset colour wedge. Note the internal tube morphology is disrupted during the calibration. The average tip pH for this tube was estimated as pH 7.2 and the growth rate was $4.7 \mu\text{m minute}^{-1}$.

potential error in this measurement caused by dye sequestration was estimated as less than 0.1 pH units assuming that 12% of the dye (see Fig. II and J) was sequestered in a compartment with a pH less than 6.0. With this colour scale a gradient of 0.3 pH units increasing from the tip would be readily visible as a transition from the speckled pattern shown in B to the mottled green and red pattern shown in B''.

pH_{cyt} and tube growth

The average cytoplasmic pH in a $20\text{--}40 \mu\text{m}^2$ region of the CZ at the tip for growing tubes was estimated as 7.11 ± 0.16 (mean \pm s.d., $n=25$; Fig. 4), using individual in situ calibrations where possible or extrapolation from in vitro calibrations, such as Fig. 3C. There was a spread in estimates of the absolute tip pH_{cyt} values between about pH 6.8 and pH 7.4, however, there was no obvious correlation of tip pH_{cyt} and growth rate (Fig. 4). For comparison, the average tip pH_{cyt} from non-growing tubes was 7.00 ± 0.21 ($n=11$).

To test whether growing tubes had cytoplasmic pH gradients, 8–32 pixel wide transects were taken along cytoplasmic regions of the tube at both wavelengths (Fig. 5A,B, data for the tube shown in Fig. 2). The average ratio was calculated from the transects (Fig. 5C) and converted to pH using the in situ calibration (Fig. 5D). The major changes in dye concentration from the 442 nm transect correspond to the low signal at the tip, possibly arising from exclusion of the dye by secretory vesicles, and a decrease in signal in the streaming cytoplasm with exclusion of the dye by larger organelles (Fig. 4A). The signal with excitation at 488 nm followed essentially the same pattern (Fig. 4B), thus the ratio was relatively constant over the first $50 \mu\text{m}$ of the tube (Fig. 4C). Estimates

of pH gradients were made separately for both the CZ and the complete tube, from the slope of linear regression after conversion of the ratio values to pH values expressed with reference to the tip. In this experiment, the slope of the regression line, expressed from tube to tip was -3.6 milli pH units μm^{-1} determined for the clear zone (the minus sign indicates a decreasing pH or acidification towards the tip) (Fig. 5D). This would correspond to an absolute pH difference of 0.043 pH units over the entire CZ, tip acid. The gradient of the regression over $50 \mu\text{m}$ of the tube was 1.2 milli pH units μm^{-1} , corresponding to an absolute pH difference of 0.06 pH units over the $50 \mu\text{m}$, confirming the absence of an apparent cytoplasmic gradient in the ratio images shown in Fig. 2B.

No consistent pH gradients were detected in the CZ (Fig. 6A) or over a $50 \mu\text{m}$ distance (Fig. 6B) in 24 other tubes. The average gradient of the regression in the clear zone spanning $15.6\pm 5.0 \mu\text{m}$ was -1.00 ± 7.88 milli pH units μm^{-1} (Fig. 6A) and 3.62 ± 5.29 milli pH units μm^{-1} for $49.5\pm 13.7 \mu\text{m}$ along the tube including the CZ (Fig. 6B). Again, there was a reasonable spread in the estimated pH gradients, however, there was no obvious correlation with growth rate for either set of measurements (Fig. 6A,B). For comparison, the gradient of the regression equations in non-growing tubes were 0.71 ± 11.47 milli pH units μm^{-1} for the CZ and 0.35 ± 4.08 milli pH units μm^{-1} for the tube.

We further investigated effects of external pH (pH_o) on pH_{cyt}, as pollen tube growth is known to depend on the pH of the growth medium. During shifts to low pH_o values, pH_{cyt} altered little, decreasing by about 0.18 pH units ($n=6$) with a 1.3 unit shift in pH_o (Fig. 7). Most tubes stopped growing, at least transiently, although cytoplasmic streaming continued. Increasing pH_o to near neutral or alkaline values was more dis-

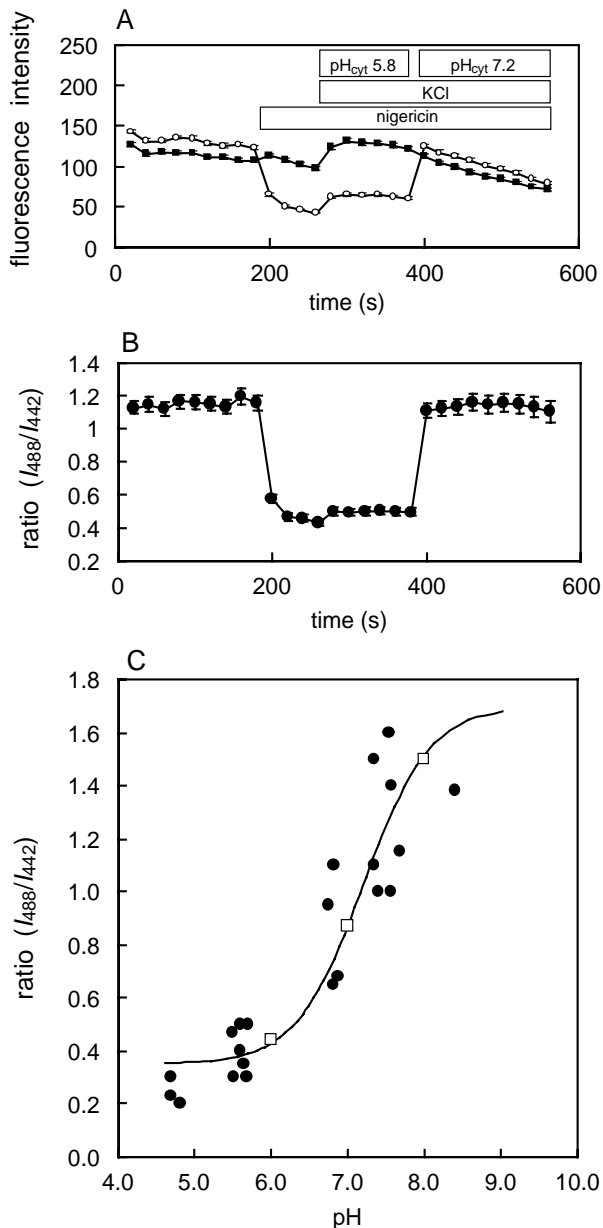


Fig. 3. In situ and in vitro pH calibrations. Average pixel values were measured for a circular $28 \mu\text{m}^2$ region at the tip of a BCECF-loaded pollen tube with excitation at 442 nm (A, closed symbols) and 488 nm (A, open symbols) during exposure to nigericin, high K^+ and varying external pH as indicated in the bars above the ratio (B). Steady-state ratio values after 2–3 minute equilibration are plotted in C along with data from 16 other similar experiments. The open symbols are data from in vitro calibrations performed using identical equipment settings. The solid line is a fit to the data using an estimated pK_a of 7.2.

ruptive: growth invariably stopped and organelles often surged towards the tip which subsequently burst (e.g. Fig. 1E–H). pH_{cyt} also shifted dramatically during transitions above a pH_0 of approx. 6.8 (Fig. 7), although few tubes remained intact to allow measurements. In such tubes the tip was observed to change most rapidly, often with a slower or no change in the main body of the tube.

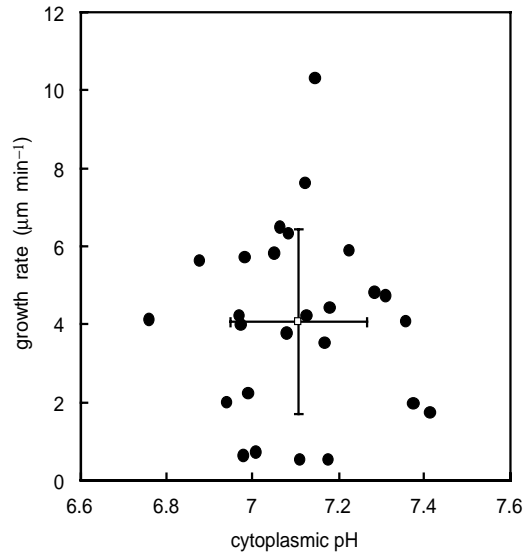


Fig. 4. Pollen tube growth rate does not correlate with tip pH. The average growth rate of 25 tubes is plotted as a function of the average tip pH. The open symbol represents the mean \pm s.d. for both variables.

Effects of plasma membrane ion transporter agonists and antagonists on tip pH and tube growth

As the plasma membrane H^+ -ATPase is the primary electrogenic pump energising the pollen tube plasma membrane, we tried to manipulate growth rate and pH_{cyt} using fusicoccin (FC), an agonist of pump activity, and sodium ortho-vanadate, a P-type ATPase inhibitor.

Addition of FC increased tube growth or caused swelling of the tip within a minute of treatment and even triggered growth in tubes that had arrested but continued to stream (e.g. Fig. 8). Such tubes provided an opportunity to test whether gradients in pH_{cyt} were associated with changes in growth rate within an individual tube. The signal with excitation at 442 nm remained evenly distributed in the cytoplasm and was excluded from larger vesicles throughout the experiment (Fig. 8A). Initially the ratio image was relatively homogeneous along the tube, and altered little over a 140 second period before addition of FC. After a lag period of about 40 seconds, the tube began to elongate rapidly and reached a nearly constant growth rate of $5.8 \mu\text{m min}^{-1}$ after a further 4 minutes. This is most clearly seen in the length-time plot (Fig. 8D) derived from the transect analysis (see Materials and Methods). Based on the calibration shown in Fig. 8E, pH_{cyt} increased by about 0.2 units at the tip after 4 minutes of FC treatment and the slope of the regression line in the CZ increased by 6.4 milli pH unit μm^{-1} (tip alkaline), corresponding to a pH gradient of about 0.16 pH units over the whole CZ (approx. $25 \mu\text{m}$, Fig. 8C). Although the tube shown in Fig. 8 was clearly growing with a slight alkaline gradient, the gradient appeared long after the change in growth rate was initiated. In addition, the average change in gradient from four such experiments was less marked (2.92 ± 4.55 milli pH units μm^{-1} , tip alkaline) for an increase in growth rate from 1.62 ± 0.98 to $4.27 \pm 1.05 \mu\text{m min}^{-1}$. The absolute tip pH_{cyt} also did not show a consistent change during FC treatment within the time frame over which effects on tube growth were observed. In Fig. 9A, data from 6 experiments

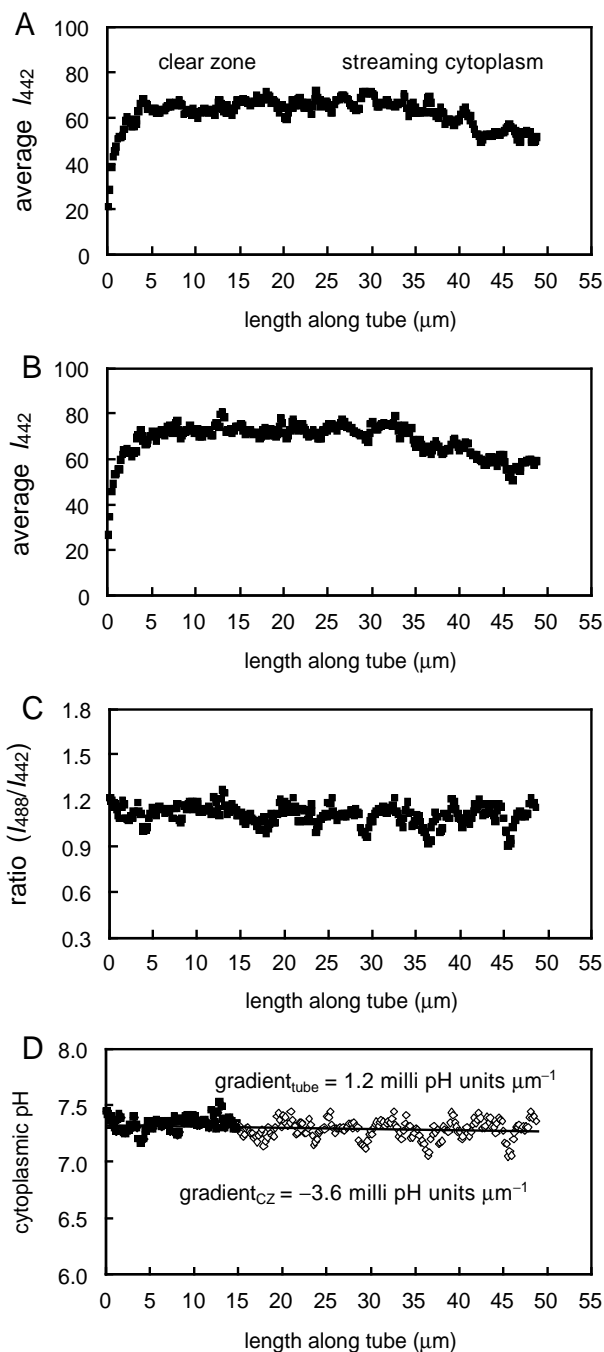


Fig. 5. Transect analysis of pH gradients in pollen tubes. A transect was drawn along the center of the pollen tube shown in Fig. 2 and the intensity averaged over 3 μm normal to the transect for the 442 nm image (A) and the 488 nm image (B). The average ratio (C) was converted to pH (D) using the in situ calibration values. pH gradients were derived by negating the slope of linear regression equations fitted to data spanning the clear zone or the entire tube over about 48 μm including the clear zone. The pH gradient is thus expressed from grain to tip.

have been normalised to the pH values immediately prior to addition of FC and expressed as the average delta pH change from this value. The average tip pH_{Cyt} varied by less than 0.1 pH unit after FC treatment.

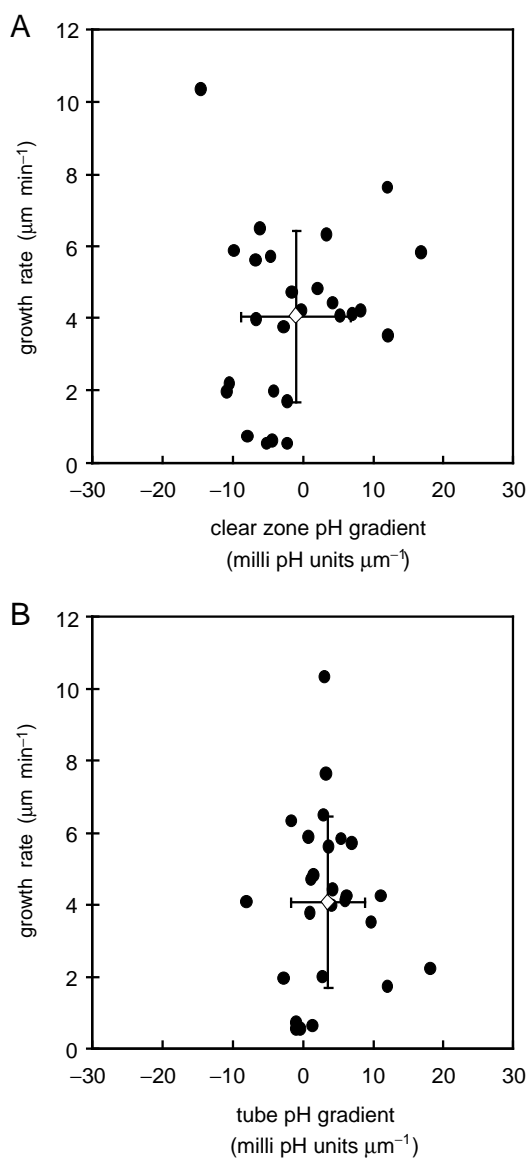


Fig. 6. Pollen tube growth does not correlate with pH gradients in the clear zone or along the tube. The average growth rate of 25 pollen tubes is plotted as a function of the pH gradient across the clear zone (A) or along the first 40–60 μm of the tube including the clear zone (B). The open symbols represent the mean \pm s.d. for both variables.

Sodium vanadate stopped growth within 60 seconds and caused a slight alkalinisation of the tip by about 0.1 pH units after 180–240 seconds (Fig. 9B; $n=8$). Addition of vanadate after FC treatment also rapidly arrested tube growth, but gave a more pronounced alkalinisation of the tip by nearly 0.2 pH units after about 80–120 seconds (Fig. 9C; $n=4$).

Effects of calcium and lanthanum on tip pH and tube growth

As an additional strategy to modify the growth rate of the pollen tubes, we tested the effect of increasing external Ca^{2+} ($[\text{Ca}^{2+}]_o$), and addition of the Ca^{2+} -channel blocker, La^{3+} , on pH_{Cyt} and tube growth, as these agents are known to modify the tip-focussed Ca^{2+} -gradients required for growth. Growth

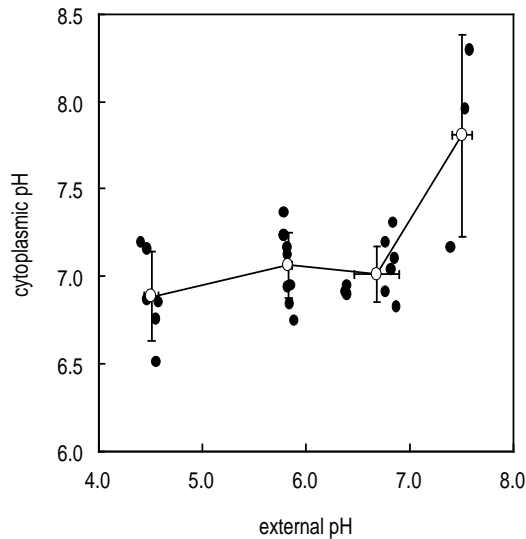


Fig. 7. Dependence of internal tip pH on external pH. The average tip pH was measured during exposure to varying external pH conditions. In time-course experiments, no marked transient changes were observed, so values are shown after 180–240 seconds equilibration at each pH. Few tubes survived pH excursions above pH 7.0; the cytoplasmic pH rapidly alkalinised and the tubes often burst. Data are taken from 9 experiments.

ceased in both treatments, however, there was no marked effect on pH_{cyt} . Increasing $[\text{Ca}^{2+}]_o$ seemed to acidify the CZ slightly, but the average pH difference was less than 0.1 pH units (Fig. 10A; $n=6$), whereas La^{3+} triggered slight and rather variable perturbations in pH_{cyt} (Fig 10B; $n=3$). Neither response was significantly different from the initial pH.

DISCUSSION

In this report, we measured the fluorescence of the pH-indicator, BCECF, after loading as the AM-ester in growing pollen tubes of *Lilium longiflorum*, using dual-excitation confocal ratio imaging. The low concentrations of AM-ester used (1–5 μM) and the cool temperature (18–20°C) appear to minimise dye sequestration in this cell type and cytoplasmic signals were readily distinguished using confocal optical sectioning. Furthermore, to increase the reliability of our measurements we used dual-excitation ratio measurements to compensate for differences in average dye concentration, dye leakage and photobleaching (e.g. Bright et al., 1987). Excitation with the 442 nm laser was particularly useful as this wavelength is close to the iso-excitation point for BCECF and the resultant image provided a direct map of the BCECF concentration. Ratio values were converted to pH values using both in situ and in vitro calibrations and gave an estimated tip pH_{cyt} of 7.11 ± 0.16 . Even with such calibrations, there is still uncertainty in the value of absolute pH reported due to the efficacy of the calibration procedures, however, differences in pH are thought to be reported reliably (see Bright et al., 1987; Read et al., 1992; Fricker et al., 1993). Accordingly, we have expressed most of our subsequent data in terms of ΔpH values.

Similar values for pH_{cyt} have been detected for other tip growing plant and algal cells, such as root hair cells, using pH-sensitive microelectrodes (pH 7.1–7.3; Herrmann and Felle, 1995), and *Pelvetia* rhizoids, using either pH-sensitive microelectrodes or dual-emission confocal ratio imaging of SNARF (pH 7.13; Gibbon and Kropf, 1994). Previous reports (Turian, 1981; Feijó et al., 1995) of pH_{cyt} measurements in pollen tubes were not calibrated. These values are at the lower end of the range reported for pH_{cyt} measured using a variety of techniques in plant (Guern et al., 1991; Felle, 1994; Fox et al., 1995; Romani et al., 1996) and algal (e.g. Bethmann et al., 1995; Gibbon and Kropf, 1993) cells, although significantly lower values have been reported in some systems (e.g. Gigliolo-Guivarc'h et al., 1996) or locally within the cytoplasm (Ross, 1992). It is possible that a lower value of pH_{cyt} is a common feature associated with tip growing systems. In the case of *Pelvetia* rhizoids, the lower absolute tip pH_{cyt} was associated with a pH gradient that increased by 0.3–0.5 pH units in a zone between 10 and 40 μm behind the tip (Gibbon and Kropf, 1994). This pH gradient was closely related to cell growth; growth was faster for higher pH gradients whereas rhizoids without any pH gradient did not grow.

A pH gradient might be anticipated in lily pollen tubes as the mechanism of tip growth is very similar in all tip-growing cells (Obermeyer and Bentrup, 1996). Indeed, a gradient of pH_{cyt} with an acidic tip and a more alkaline pH in the cytoplasm behind the tip was reported in preliminary studies (Turian, 1981; U. K. Tirlapur as cited by Pierson and Cresti, 1992). However, in this study no consistent pH gradients were detected in growing lily pollen tubes by inspection of the ratio images or quantitative analysis of transects along the tubes. Furthermore the absolute tip pH_{cyt} did not correlate with the rate of tube growth. We infer from these results that tip-acid pH gradients are not a prerequisite for tip growth in this system.

Although our experimental approach minimised any effects of dye compartmentalisation into the tubular network and large organelles, we cannot exclude the formal possibility that BCECF was sequestered into a sub-resolution compartment(s) and this obscured a genuine cytoplasmic pH gradient. If these vesicles were distributed evenly and the volume fraction and/or dye concentration resulted in a substantially greater signal than that from the cytoplasm, then longitudinal differences in cytoplasmic pH would be suppressed. The pH reported would essentially refer to the pH of the sub-resolution compartment. However, quantitation of the level of sequestration indicated that typically less than 12% of the dye was in vesicles and would not therefore be sufficient to mask a cytoplasmic pH gradient. Alternatively, if the dye were sequestered in a population of asymmetrically distributed vesicles, the dye concentration, compartment pH and vesicle distribution could give rise to a signal that exactly counterbalanced the 'true' cytoplasmic pH gradient in that region. To explain our data using this model, the BCECF concentration, sub-cellular distribution and compartment pH would have to have balanced the cytoplasmic signal at all the growth rates observed, including in non-growing tubes. Furthermore, the balance would have to have been maintained for extended periods of growth in individual pollen tubes, with variable levels of dye loading in the population and under particular treatments, such as stimulation of growth by fusicoccin. On balance, this explanation does not appear likely.

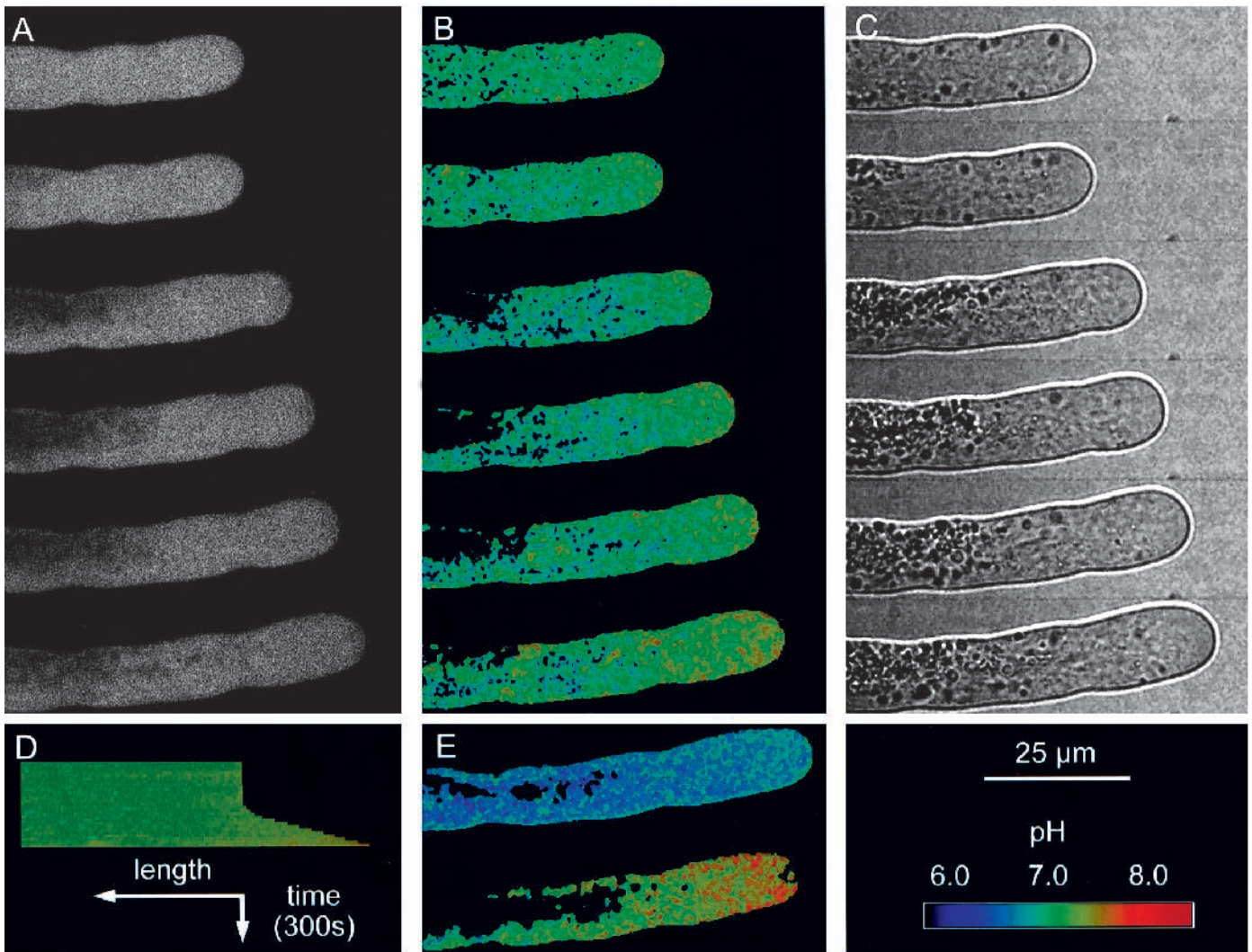


Fig. 8. Effects of fusicoccin on pollen tube growth and cytoplasmic pH in growing pollen tubes of *Lilium longiflorum*. Fusicoccin stimulated pollen tube growth, but had no consistent effect on pH_{cyt} . In this example fusicoccin stimulated rapid growth of an initially non-growing tube to a value of $5.8 \mu\text{m minute}^{-1}$. There was no marked pH gradient along the tube (B) either when it was not growing or during the early stages of fusicoccin-stimulated growth. This is most clearly seen in the length-time plot derived from the transect analysis (D). After about 4 minutes in fusicoccin, the tip pH had increased by about 0.2 pH units, by comparison with in situ calibration at pH 6.7 and pH 7.3 (E). A slight pH gradient of similar magnitude (0.16 pH units) was present across the clear zone, with the tip more alkaline than the body of the tube. The average pH gradient in 4 such experiments was less than 0.1 pH unit. (Imaging conditions as for Fig. 2 except that the time-interval between image sets was 140 seconds for the first two images followed by a gap of 240 seconds and 40 seconds thereafter).

Measurements of pH_{cyt} in growing root hairs of *Sinapis alba* also failed to detect any pH gradients and changes in pH_{cyt} had only a marginal influence on the rate of hair elongation (Herrmann and Felle, 1995). In a recent survey of several tip growing systems including fern rhizoids (Parton, 1996), fungal hyphae and pollen tubes, there was no evidence that pH gradients were required for growth (Parton et al., 1997). Thus, although pH_{cyt} gradients may occur in particular species, the current evidence does not support a universal requirement for such gradients in the organisation or maintenance of tip growth. This is in contrast to the situation for Ca^{2+} ions, where tip-focussed gradients appear to be essential for tip growth (Nobiling and Reiss, 1987; Obermeyer and Weisenseel, 1991; Rathore et al., 1991; Pierson et al., 1995).

pH_{cyt} regulation

Although gradients in pH_{cyt} do not appear to be critical in regulation of tip growth in pollen tubes, tube growth and tip pH_{cyt} were very sensitive to alkalinisation of the external medium to values exceeding about pH 7. The normal physiological pH of the apoplast of the stigmatic surface or stylar tissues is not known, however, in other arial tissues estimates of apoplastic pH are spread over a wide range between pH 4.8 and pH 7.2 (e.g. Edwards et al., 1988; Mühling et al., 1995; Peters, and Felle, 1991), depending to a large extent on the level of proton extrusion around each cell type. Interestingly, apoplastic pH is reported to increase under certain stress conditions (Hartung and Slovik, 1991) and may therefore influence pollen tube growth in vivo. In the pH_0

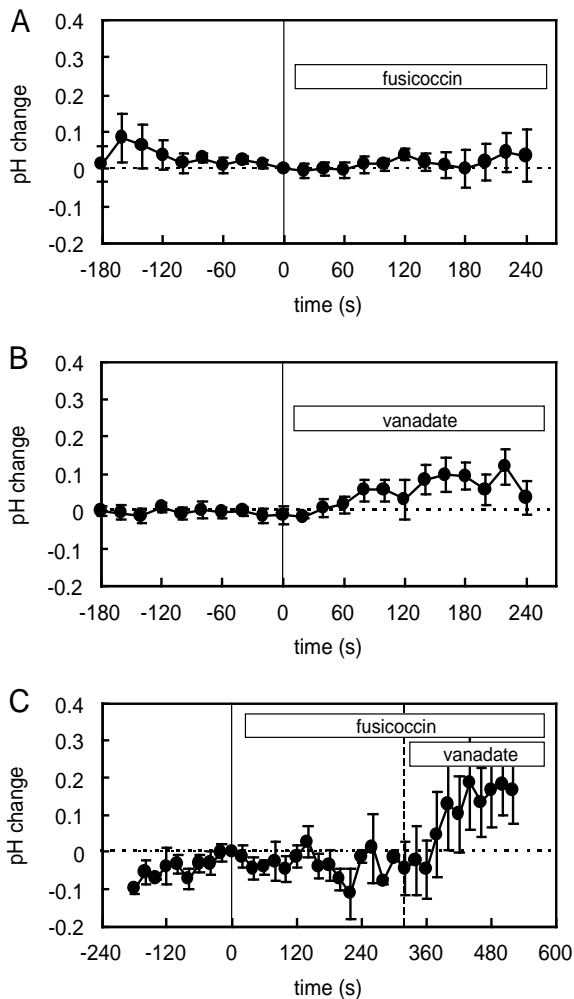


Fig. 9. Effects of plasma membrane H⁺-ATPase agonists and antagonists on pH_{cyt}. Changes in the average tip pH_{cyt} were measured during treatment with the PM H⁺-ATPase agonist, fusicoccin (A), the PM H⁺-ATPase inhibitor, vanadate alone (B) or during FC treatment (C). Results are normalised to the pH value immediately prior addition of the first stimulus and represent the mean ± s.e.m. *n*=6 (A), *n*=8 (B) and *n*=4 (C).

range of pH 4.5–7.0, pollen tubes were able to maintain a relatively constant pH_{cyt} and did not even show transient pH changes in response to step-wise decreases in p*H*_o of up to 1.3 pH units. We infer from this data that mechanisms exist to rapidly compensate for H⁺-influx at the tip and sub-tip, although such mechanisms must exclude the action of the PM ATPase as this localises to the pollen grain (Obermeyer et al., 1992).

It has been shown that the plasma membrane (PM) H⁺-ATPase is important for pollen tube growth and components affecting pump activity also change the pollen tube growth rate, e.g. fusicoccin, boron and AC fields of low frequency stimulated pollen tube growth by increasing the activity of the PM H⁺-ATPase (Rodríguez-Rosales et al., 1989; Obermeyer et al., 1996; Plätzer et al., 1997). In this study, addition of fusicoccin did not consistently change the tip pH_{cyt}, but appeared to increase the rate of growth, manifest as either an increase in linear extension rate or as rapid and extensive swelling of the

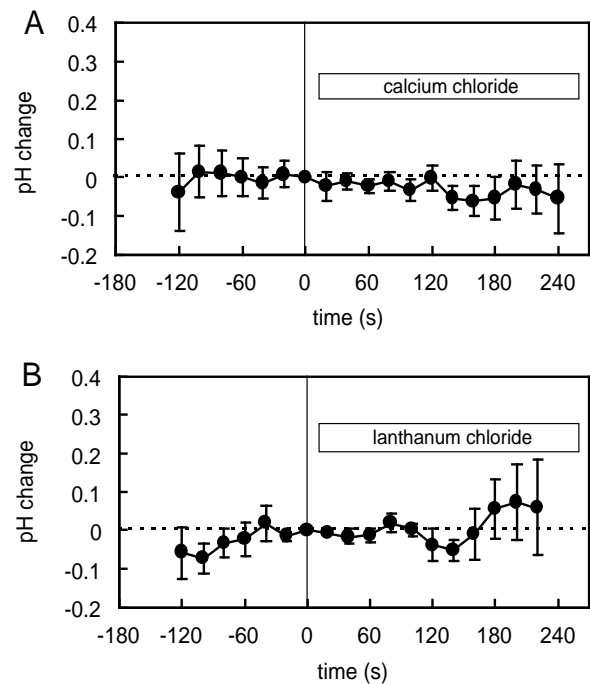


Fig. 10. Effects of Ca²⁺ and La³⁺ on tip pH_{cyt}. Changes in the average tip pH_{cyt} were measured during treatment with Ca²⁺ (A) or the Ca²⁺-channel blocker, La³⁺ (B). Results are normalised to the pH value immediately prior to addition of the stimulus and represent the mean ± s.e.m., *n*=8 (A) and *n*=3 (B).

tube tip. Application of vanadate, an inhibitor of the PM H⁺-ATPase, arrested pollen tube growth and caused a slight alkalinisation of the tip cytoplasm (Fig. 9B). This vanadate-induced alkalinisation was higher when the PM H⁺-ATPase was first stimulated by fusicoccin (Fig. 9C). These results are consistent with the observed distribution of the PM H⁺-ATPase (Obermeyer et al., 1992) and the protonic circuit exiting the grain and re-entering along the pollen tube and at the tip (Weisenseel and Jaffe, 1976). During normal growth, H⁺-influx, possibly via sucrose/*n*H⁺ symporter activity, would be matched by sequestration into other compartments, dispersion in the streaming cytoplasm and/or metabolic consumption. In this model, the alkalinisation observed at the tip after inhibition of the pump by vanadate would thus reflect the dominance of the H⁺-removal machinery, as the net PM H⁺-influx declined in this region. This effect would be more pronounced after FC stimulation of the pump if the system had previously accommodated the increased flux.

Conclusions

In summary, our data do not support a central role for tip-acid pH gradients in organisation or maintenance of the structures leading to tip growth in pollen tubes. However, the absolute value of the tip pH_{cyt} appears to be marginally lower than pH_{cyt} in other non-tip growing cell types and may therefore have some as yet undefined significance. The effects of various agonists and antagonists also indicate that the mechanisms that would normally stabilise pH_{cyt} are spatially separated in this highly polarised tip-growing system. Experiments with changing external pH, fusicoccin and vanadate all lend support

to the idea that pH homeostasis at the tip may normally require a proton influx. Interruption of the steady state H^+ -flux leads to substantial alkalinisation of pH_{Cyt} and growth arrest or even tube-bursting.

G.O. thanks the British Council for travel grants. N.S.W. is a Royal Society Industry Fellow. Equipment used in this work was purchased using SERC grants to M.D.F. and N.S.W., and Royal Society, AFRC and Nuffield Foundation grants to M.D.F. M.D.F. and N.S.W. thank R. J. Errington for many helpful discussions.

REFERENCES

- Bethmann, B., Thaler, M., Simonis, W. and Schönknecht, G. (1995). Electrochemical potential gradient of H^+ , K^+ , Ca^{2+} , and Cl^- across the tonoplast of the green alga *Eremosphaera viridis*. *Plant Physiol.* **109**, 1317-1326.
- Blackbourn, H. D., Walker, J. H. and Battey, N. H. (1991). Calcium-dependent phospholipid binding proteins in plants. Their characterisation and potential for regulating cell growth. *Planta* **184**, 67-73.
- Blackbourn, H. D., Barber, P. J., Huskisson, N. S. and Battey, N. H. (1992). Properties and partial protein sequence of plant annexins. *Plant Physiol.* **99**, 864-871.
- Bright, G. R., Fisher, G. W., Rogowska, J. and Taylor, D. L. (1987). Fluorescence ratio imaging microscopy: temporal and spatial measurements of cytoplasmic pH. *J. Cell Biol.* **104**, 1019-1033.
- Cai, G., Moscatelli, A., del Casino, C. and Cresti, M. (1996). Cytoplasmic motors and pollen tube growth. *Sex. Plant Reprod.* **9**, 59-64.
- Chaillet, J. R. and Boron, W. F. (1985). Intracellular calibration of a pH-sensitive dye in isolated, perfused salamander proximal tubules. *J. Gen. Physiol.* **86**, 765-794.
- Derksen, J., Rutten, T., van Amstel, T., de Win, A., Doris, F. and Steer, M. (1995). Regulation of pollen tube growth. *Acta Bot. Neerl.* **44**, 93-119.
- Edwards, M. C., Smith, G. N. and Bowling, D. J. F. (1988). Guard cells extrude protons prior to stomatal opening - a study using fluorescence microscopy and pH micro-electrodes. *J. Exp. Bot.* **39**, 1541-1547.
- Feijó, J. A., Malhó, R. and Obermeyer, G. (1995). Ion dynamics and its possible role during in vitro pollen germination and tube growth. *Protoplasma* **187**, 155-167.
- Felle, H. H. (1994). The H^+/Cl^- symporter in root-hair cells of *Sinapis alba*. An electrophysiological study using ion-selective electrodes. *Plant Physiol.* **106**, 1131-1136.
- Fox, G. G., McCallan, N. R. and Ratcliffe, R. G. (1995). Manipulating cytoplasmic pH under anoxia: A critical test of the role of pH in the switch from aerobic to anaerobic metabolism. *Planta* **195**, 324-330.
- Fricke, M. D. and White, N. S. (1992). Wavelength considerations in confocal microscopy of botanical specimens. *J. Microsc.* **166**, 29-42.
- Fricke, M. D., Tester, M. and Gilroy, S. G. (1993). Fluorescent and luminescent techniques to probe ion activities in living plant cells. In *Fluorescent and Luminescent Probes for Biological Activity: A Practical guide to Technology for Quantitative Real-Time Analysis* (ed. W. T. Mason), pp. 361-378. Academic Press, London.
- Fricke, M. D., Tlalka, M., Ermantraut, J., Obermeyer, G., Dewey, M., Gurr, S., Patrick, J. and White, N. S. (1994). Confocal fluorescence ratio imaging of ion activities in plant cells. *Scan. Microsc.* (suppl.) **8**, 391-405.
- Fricke, M. D., Errington, R. J., Wood, J. L., Tlalka, M., May, M. and White, N. S. (1997). Quantitative confocal fluorescence measurements in living tissues. In *Signal Transduction - Single Cell Techniques* (ed. B. Van Duijn). Springer-Verlag, Heidelberg (in press).
- Gibbon, B. C. and Kropf, D. L. (1993). Intracellular pH and its regulation in *Pelvetia zygotes*. *Dev. Biol.* **157**, 259-268.
- Gibbon, B. C. and Kropf, D. L. (1994). Cytosolic pH gradients associated with tip growth. *Science* **263**, 1419-1421.
- Gigliolo-Guivarc'h, N., Pierre, J.-N., Vidal, J. and Brown, S. (1996). Flow cytometric analysis of cytosolic pH of mesophyll cell protoplasts from the crabgrass *Digitaria sanguinalis*. *Cytometry* **23**, 241-249.
- Guern, J., Felle, H., Matthieu, Y. and Kurdjian, A. (1991). Regulation of intracellular pH in plant cells. *Int. Rev. Cytol.* **127**, 111-173.
- Hartung, W. and Slovik, S. (1991). Physicochemical properties of plant growth regulators and plant tissues determine their distribution and redistribution: stomatal regulation by abscisic acid in leaves. *New Phytol.* **119**, 361-382.
- Haußer, I., Herth, W. and Reiss, H.-D. (1984). Calmodulin in tip growing plant cells, visualized by fluorescing calmodulin-binding phenothiazines. *Planta* **162**, 33-39.
- Herrmann, A. and Felle, H. H. (1995). Tip growth in root hair cells of *Sinapis alba* L.: Significance of internal and external Ca^{2+} and pH. *New Phytol.* **129**, 523-533.
- Heslop-Harrison, J. and Heslop-Harrison, Y. (1989). Myosin associated with the surface of organelles, vegetative nuclei and generative cells in angiosperm pollen grains and tubes. *J. Cell Sci.* **94**, 319-325.
- Kohn, T. and Shimmen, T. (1987). Ca^{2+} -induced fragmentation of actin filaments in pollen tubes. *Protoplasma* **141**, 177-179.
- Kühtreiber, W. M. and Jaffe, L. F. (1990). Detection of extracellular calcium gradients with a calcium-specific vibration electrode. *J. Cell Biol.* **110**, 1505-1573.
- Lancelli, S. A. and Hepler, P. K. (1992). Ultrastructure of freeze-substituted pollen tubes of *Lilium longiflorum*. *Protoplasma* **167**, 215-230.
- Miller, D. D., Callaham, D. A., Gross, D. J. and Hepler, P. K. (1992). Free Ca^{2+} gradient in growing pollen tubes of *Lilium*. *J. Cell Sci.* **101**, 7-12.
- Malhó, R., Read, N. D., Trewavas, A. J. and Pais, S. M. (1995). Calcium channel activity during pollen tube growth and reorientation. *Plant Cell* **7**, 1173-1184.
- McGillivray, A. M. and Gow, N. A. R. (1987). The transhyphal electrical current of *Neurospora crassa* is carried principally by protons. *J. Gen. Microbiol.* **133**, 2875-2881.
- Mühling, K., Plieth, C., Hansen, U.-P. and Sattelmacher, B. (1995). Apoplastic pH of intact leaves of *Vicia faba* as influenced by light. *J. Exp. Bot.* **46**, 377-382.
- Nobiling, R. and Reiss, H.-D. (1987). Quantitative analysis of calcium gradients and activity in growing pollen tubes of *Lilium longiflorum*. *Protoplasma* **139**, 20-24.
- Obermeyer, G. and Weisenseel, M. H. (1991). Calcium channel blocker and calmodulin antagonists affect the gradient of free calcium ions in lily pollen tubes. *Eur. J. Cell Biol.* **56**, 319-327.
- Obermeyer, G., Lützelshwab, M., Heumann, H.-G. and Weisenseel, M. H. (1992). Immunolocalization of H^+ -ATPases in the plasma membrane of pollen grains and pollen tubes of *Lilium longiflorum*. *Protoplasma* **171**, 55-63.
- Obermeyer, G. and Blatt, M. R. (1995). Electrical properties of intact pollen grains of *Lilium longiflorum*: Characteristics of the non-germinating pollen grain. *J. Exp. Bot.* **46**, 803-813.
- Obermeyer, G. and Bentrup, F.-W. (1996). Regulation of polar cell growth and morphogenesis. *Progr. Bot.* **57**, 54-67.
- Obermeyer, G., Kriechbaumer, R., Strasser, D., Maschessnig, A. and Bentrup, F.-W. (1996). Boric acid stimulates the plasma membrane H^+ ATPase of ungerminated lily pollen grains. *Physiol. Plant.* **98**, 281-290.
- Parton, R. (1996). PhD thesis. University of Edinburgh.
- Parton, R., Fischer, S., Malhó, R., Jelitto, T. C. and Read, N. R. (1997). Pronounced cytoplasmic pH gradients are not required for tip growth in plant and fungal cells. *J. Cell Sci.* **110**, 1187-1198.
- Peters, W. and Felle, H. (1991). Control of apoplast pH in corn coleoptile segments. I: The endogenous regulation of cell wall pH. *J. Plant Physiol.* **137**, 655-661.
- Picton, J. M. and Steer, M. W. (1983). Membrane recycling and the control of secretory activity in pollen tubes. *J. Cell Sci.* **63**, 303-310.
- Pierson, E. S. and Cresti, M. (1992). Cytoskeleton and cytoplasmic organisation of pollen and pollen tubes. *Int. Rev. Cytol.* **140**, 73-128.
- Pierson, E. S., Miller, D. D., Callaham, D. A., Shipley, A. M., Rivers, B. A., Cresti, M. and Hepler, P. K. (1995). Pollen tube growth is coupled to the extracellular ion flux and the intracellular calcium gradient: Effect of BAPTA-type buffers and hypertonic media. *Plant Cell* **6**, 1815-1828.
- Plätzer, K., Obermeyer, G. and Bentrup, F.-W. (1997). AC fields of low frequency and amplitude stimulate pollen tube growth possible via stimulation of the plasma membrane proton pump. *Bioelectrochem. Bioenerg.* (in press).
- Putnam-Evans, C., Harmon, A. C., Palevitz, B. A., Fechheimer, M. and Cormier, M. J. (1989). Calcium-dependent protein kinase is localized with F-actin in plant cells. *Cell Mot. Cytoskel.* **12**, 12-22.
- Rathore, K. S., Cork, R. J. and Robinson, K. R. (1991). A cytoplasmic gradient of Ca^{2+} is correlated with the growth of lily pollen tubes. *Dev. Biol.* **148**, 612-619.
- Read, N. D., Allen, W. T. G., Knight, H., Knight, M. R., Malho, R., Russell,

- A., Shacklock, P. S. and Trewavas, A. J.** (1992). Imaging and measurement of cytosolic free calcium in plant and fungal cells. *J. Microsc.* **166**, 57-86.
- Reiss, H.-D. and Herth, W.** (1979). Calcium ionophore A23187 affects localized wall secretion in the tip region of pollen tubes of *Lilium longiflorum*. *Planta* **145**, 225-232.
- Rodriguez-Rosales, M. P., Roldán, M., Belver, A. and Donaire, J. P.** (1989). Correlation between in vitro germination capacity and proton extrusion in olive pollen. *Plant Physiol. Biochem.* **27**, 723-728.
- Romani, G., Beffanga, N. and Meraviglia, G.** (1996). Role for the vacuolar H⁺-ATPase in regulating the cytoplasmic pH: An in vivo study carried out in chl1, an *Arabidopsis thaliana* mutant impaired in NO₃⁻ transport. *Plant Cell Physiol.* **37**, 285-291.
- Ross, W.** (1992). Confocal pH topography in plant cells: acidic layers in the peripheral cytoplasm and the apoplast. *Bot. Acta* **105**, 253-259.
- Russ, U., Grolig, F. and Wagner, G.** (1991). Changes in cytoplasmic free Ca²⁺ in the green alga *Mougeotia scalaris* as monitored with Indo-1, and their effects on the velocity of chloroplast movements. *Planta* **184**, 105-112.
- Tirlapur, U. K., Scali, M., Moscatelli, A., Del Casino, C., Cai, G., Tiezzi, A. and Cresti, M.** (1994). Confocal image analysis of spatial variations in immunocytochemically identified calmodulin during pollen hydration, germination and pollen tube tip growth in *Nicotiana tabacum* L. *Zygote* **2**, 63-68.
- Tiwari, S. C. and Suprenant, K. A.** (1994). pH-dependent solubility and assembly of microtubules in bovine brain extracts. *Cell Motil. Cytoskel.* **28**, 69-78.
- Turian, G.** (1981). Decreasing pH-gradient toward the apex of germinating pollen tubes. *Bot. Helv.* **91**, 161-167.
- Turian, G., Ton-That, T. C. and Ortega-Perez, R.** (1985). Acid tip linear growth in the fungi: Requirements for H⁺/Ca²⁺ inverse gradients and cytoskeleton integrity. *Bot. Helv.* **95**, 311-322.
- VanDerWoude, W. J., Morré, D. J. and Bracker, C. E.** (1974). Isolation and characterisation of secretory vesicles in germinated pollen of *Lilium longiflorum*. *J. Cell Sci.* **8**, 331-351.
- Weisenseel, M. H. and Jaffe, L. F.** (1976). The major growth current through lily pollen enters as K⁺ and leaves as H⁺. *Planta* **133**, 1-7.

(Received 6 December 1996 - Accepted 9 May 1997)